Preprint
UCRL-JC-148580

Mechanisms of CO_2 Laser Mitigation of Laser Damage Growth in Fused Silica

M.D. Feit, A.M. Rubenchik

This article was submitted to the Boulder Damage Symposium XXXXIV: Annual Symposium on Optical Materials for High Power Lasers, Boulder, Colorado, September 16-18, 2002

September 5, 2002

U.S. Department of Energy
Lawrence Livermore National Laboratory

DISCLAIMER

This work was performed under the auspices of the U. S. Department of Energy by the University of California, Lawrence Livermore National Laboratory under Contract No. W-7405-Eng-48.

Mechanisms of CO_2 laser mitigation of laser damage growth in fused silica

M.D. Feit* and A.M. Rubenchik
Lawrence Livermore National Laboratory, P.O. Box 808- L-491, Livermore, CA 94550

ABSTRACT

Theoretical models for heating, evaporation, material flow, and stress and strain generation accompanying CO_2 laser damage mitigation and surface treatment of fused silica are developed to aid understanding of scaling with process parameters. We find that lateral nonlinear heat transport is an important cooling mechanism, more significant than evaporative cooling. Scaling laws relating experiments with different set of parameters are presented. Transverse conduction, together with the increased thermal conductivity at high temperatures, allows a gentle evaporation regime at low laser intensity in which the rate can be controlled via laser fluence. For higher laser intensity, recoil momentum imparted by rapid evaporation generates pressure, which can lead to transverse flow of the melted material. Only a very thin layer can flow because viscosity increases rapidly with depth. Evaporation and flow are subject to instabilities that can impact surface quality, especially surface flatness, if large areas are processed. Also material flow can heal cracks and improve material quality. Analysis of stress indicates that maximal tensile stresses of order 0.1 GPa, comparable to the tensile strength, can be generated.

Keywords: laser damage growth, fused silica, laser mitigation

1. INTRODUCTION

Since the discovery[1] that the transverse size of laser-induced damage in fused silica grows exponentially with repeated laser exposures, it has been evident that damage growth is the key factor in determining beam obscuration and scattering losses resulting from laser-induced damage. Growth mitigation is needed to limit these losses for the large optics used in high-power lasers. Various approaches have been investigated[2] including chemical etch, plasma etch, and CO_2 laser treatment. The CO_2 treatment of individual damage sites has proven the most effective. It was noted[3] by the end of the 1970's that exposure of fused silica to CO_2 laser radiation could lead to increased damage resistance. It was concluded this effect probably implied healing of sub-surface fracture. This conclusion was strengthened by the observation[4] that increased damage resistance occurred at a fairly sharp laser power transition and probably corresponded to temperatures at which flow begins as evidenced by residual strains left in the material. This early work dealt with small beam damage. It is interesting to note that both the above[5 -6]and other[7] early workers in laser cleaning noted that CO_2 laser processed silica surfaces had reduced water and hydrocarbon content compared with mechanically polished surfaces.

More recent experiments[2] have demonstrated successful mitigation of growth of laser-initiated damage spots on large silica optics using CO_2 laser irradiation. Indeed, the optical strength of material around the mitigated spot can be even higher than in the pristine material. These results make this mitigation method attractive for large-scale mitigation of NIF optics and motivate theoretical studies of the mitigation process to determine process scaling and optimization. We find that the laser radiation not only evaporates the damaged material, but also heals microcracks. The present paper summarizes our theoretical understanding of CO_2 laser-damage mitigation.

Growth of the damage spot is associated with enhanced absorption in material modified after previous laser shots. The ideal mitigation scheme must include local heating of the damage spot, melting and evaporation or revitrification of the modified material. Even if the transformation of heated modified material back to

*Correspondence: Email: feit1@llnl.gov; Telephone: 925-422-2418: Fax: 925-422-5718

fused silica is quick, some time is required for closure of voids and microcracks. Due to the large viscosity of fused silica, such closure is made possible only by heating the material up to high temperature: temperature high enough that significant evaporation of material is inevitable. Both evaporation and material healing are very sensitive to temperature, so temperature modeling is essential for an evaluation of the mitigation process.

In most of the experiments done to date, the laser pulse is too short for the steady state to be reached so the nonstationarity of the temperature distribution is important. The effects of nonstationarity will be discussed in the next section of the paper.

The evaporation rate is very sensitive to the surface temperature, which therefore must be evaluated as accurately as possible. As a result, the nonlinearity (temperature dependent conductivity) of thermal conduction must be taken into account[8]. We will discuss a convenient scaling law to relate experiments with different parameters.

The enhanced optical strength of mitigated spots can be attributed to the healing of microcracks in the surrounding material. We will estimate the extent of the zone where material improvement takes place. We discuss thermal stresses induced by laser heating and the way to minimize their detrimental effects.

Finally, implications of these results for optimal mitigation strategy will be discussed.

2. NONSTATIONARY TEMPERATURE EFFECTS

We discuss here the role of temperature nonstationarity disregarding the temperature dependence of the thermal conductivity. The role of such nonlinearity will be discussed semi-quantitatively later.

The temperature distribution on the surface of an optic induced by a Gaussian laser beam is given by the expression[9]

$$T(r,t)=\frac{Aa^2}{D}\sqrt{\frac{\kappa}{\pi}}\int_0^t \frac{I(t-\tau)}{\sqrt{\tau}\left(a^2+4D\tau\right)} e^{-\frac{r^2}{a^2+4D\tau}}\, d\tau \qquad (1)$$

where A is the absorbed fraction, A=0.85 for fused silica irradiated by a CO_2 laser, D is the thermal diffusivity and κ is the thermal conduction coefficient. The intensity of the laser beam is $I(r,t)=I(t)\exp[-r^2/a^2]$. For a flat-top temporal pulse with duration τ and constant intensity I, the temperature at the center of the laser spot is

$$T=\frac{0.85P}{(\pi)^{3/2}a\kappa}Arc\tan\left(\sqrt{\frac{t}{\tau}}\right) \qquad with \quad \tau=\frac{a^2}{4D} \qquad (2)$$

Here $P = I\pi a^2$ is the beam power. Asymptotically, the temperature in the center of the laser spot approaches the stationary value T_s.

$$T_s=\frac{0.85P}{2a\kappa\sqrt{\pi}}=0.24\frac{P}{a\kappa} \qquad (3)$$

The surface temperature determines the ablation rate[10]. The velocity of the evaporation front is given by the expression[10]

$$V=V_0 e^{-U/kT} \tag{4}$$

where U is the latent heat of evaporation per atom, U=3.6 eV for fused silica and $V_0=3.8 \times 10^5$ cm/s.

Temporal evolution of temperature and ablation rates are shown in Fig.(1) for the case where the steady-state temperature is 2245°K and the steady state ablation rate is 50μ/s. One can see that the onset of the steady state regime for temperature is fast, about 10 $a^2/4D$. Of course, the temperature is slightly different from the asymptotic value for a long time. Even at t=100 $a^2/4D$, the temperature reaches only 0.94 of the steady state value. The ablation rate, however, is very sensitive to temperature, and, at the temperature at t=100 $a^2/4D$, is only 14.4 μm/s compared to 50 μm/s at steady state. Thus, the ablation steady state is much harder to reach than the temperature steady state.

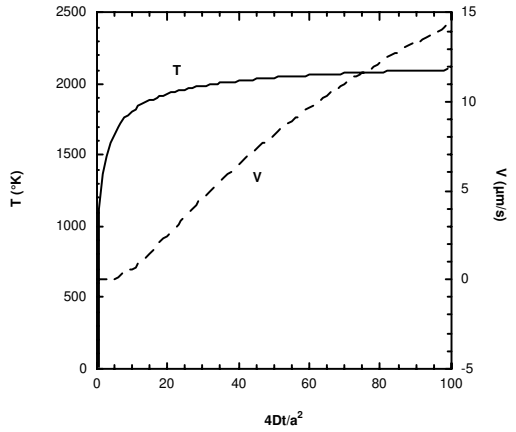

Fig.1: Temporal evolution of the temperature and ablation rate at the center of the laser spot. Time is measured in units of the thermal time $a^2/4D$.

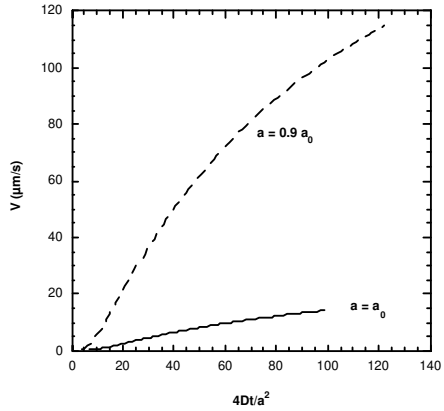

Fig.2: Ablation rate evolution for beam radii a_0 and $0.9a_0$ for same conditions as above.

As a result, the ablation rate is very sensitive to small variations of beam parameters, i.e. spot size and power. The temperature is dependent on beam size of course. The larger sensitivity of the ablation rate to small variations in beam size is shown in Fig(2).

An important effect not taken into account thus far is the nonlinearity of thermal conduction, which reduces the sensitivity of the ablation rate to variation in the processing parameters[8]. Increase of thermal conductivity at high temperatures shortens the onset of the steady state; nevertheless, one can expect that the mitigation process typically will take place in the nonstationary ablation regime.

3. NONLINEARITY OF THERMAL CONDUCTION AND SCALING LAW

The thermal conductivity of silica increases with temperature. Above about 800K, the effective conductivity (rate at which thermal energy is lost) is determined mostly by radiation transport[11]. We will use the following empirical interpolation formula for the thermal conductivity of fused silica:

$$\kappa(T) = \kappa_0 + \beta T^3 = 0.01(1 + 1.7 \cdot 10^{-9} T^3)(W/cmK) = \kappa_0 f(\frac{T}{T_0}) \tag{5}$$

The coefficient β is determined from experimental data, κ_0=0.01 W/cm°K at room temperature, κ~0.04 W/cm°K at T_0=1200°K. It must be mentioned that the experimental data is not very detailed. As far as the

contribution of radiation transport is concerned, some photons traverse the sample without absorption and the effective thermal conduction can then depend on sample shape. As a result, experimental information on effective thermal conduction is not very reliable and should be used for qualitative estimates only. For simplicity below, we disregard the temperature dependence of density and specific heat, which is not essential.

For $T<<T_0$ thermal transport can be treated as linear, i.e. $\kappa(T)= \kappa_0$. In the opposite case one can put

$$\kappa(T) = \beta T^3 = 0.01(1.7x10^{-9}T^3)(W/cmK) = \kappa_0(\frac{T}{T_0})^3 \qquad (6)$$

The simple power law dependence of Eq.(6) affords a chance to find a scaling relation even in the highly nonlinear regime.

We must solve the thermal diffusion equation

$$\rho c\frac{\partial T}{\partial t} = \nabla \bullet (\kappa(T)\nabla T) \qquad (7)$$

with the boundary condition

$$-\kappa(T)\frac{\partial T}{\partial z} = AIe^{-\frac{r^2}{a^2}} \qquad at \quad z = 0 \qquad (8)$$

If we normalize spatial scales by the beam radius a, and introduce the dimensionless diffusion time Dt/a^2, where $D=\kappa_0/\rho c$, one sees that the problem will be characterized by one dimensionless parameter $s= AIa/\kappa_0 T_0$. Here T_0 is a specific temperature scale introduced in Eq.(5). This implies that the surface temperature and the ablation rate are functions of P/a and dimensionless time only. That is, surface temperature can be written in the form

$$T = T_0 f(\frac{AP}{a\kappa_0 T_0}, \frac{r}{a}, \frac{Dt}{a^2}) \qquad (9)$$

where the structure of the function f is determined by the nonlinearity of thermal conduction. Let parameter s be the ratio of the surface temperature to T_0 for the case of linear thermal conduction. In the regime with nonlinear thermal conduction, $s>>1$, the relation Eq.(9) then offers the possibility to rescale experiments with different parameters. For example, to have the same processed crater for a beam spot two times larger, one must not only increase the power two times, but also increase pulse duration four times.

For $s>>1$, when thermal conduction can be adequately described by Eq.(6) instead of Eq.(9) one can derive a simpler scaling

$$T = T_0 s^{1/4} f\left(\frac{r}{a}, \frac{Dts^{3/4}}{a^2}\right); \qquad s = \frac{AP}{aT_0\kappa_0} \qquad (10)$$

One can think of this as an increase of the effective thermal diffusivity at high power.
For thermal conduction of a more general type, $\kappa=\kappa_0(T/T_0)^n$ the scaling takes the form

$$T = T_0 s^{1/n+1} f\left(\frac{r}{a}, \frac{Dts^{n/n+1}}{a^2}\right); \qquad s = \frac{AP}{aT_0\kappa_0}$$

From Eq.(10), one sees that as power increases, surface temperature increases as $P^{1/4}$ and time for the temperature onset decreases as $P^{-3/4}$.

We introduce the new variable u,

$$\kappa_0 u = \int_0^T \kappa(T) dT \tag{11}$$

Equation (11), with boundary condition Eq.(8), can be rewritten as

$$\frac{\partial T}{\partial t} = D\Delta u; \qquad -\kappa_0 \frac{\partial u}{\partial z} = AI(r)\,|_{z=0} \tag{12}$$

One can see that in the steady-state situation the equations for u and for the temperature with temperature independent thermal conduction are identical, and for u in the center of the laser spot we have the analog of Eq.(3)

$$u_s = \frac{0.85P}{2ak_0\sqrt{\pi}} = 0.24\frac{P}{ak_0} \tag{13}$$

For the thermal conduction law (2.2) we find for the temperature in the center of the laser spot

$$T = 0.75T_0\left(\frac{P}{a\kappa_0 T_0}\right)^{1/4}$$

In Fig.(3) we compare the calculated evaporation rates vs. beam power both for linear thermal conduction, and for thermal transport described by Eq.(5) with experiment. The beam size was used as a fit parameter at a power of 50 W. The steepness of the curves is at issue here. One sees that Eq.(5) gives a better fit to experiment.

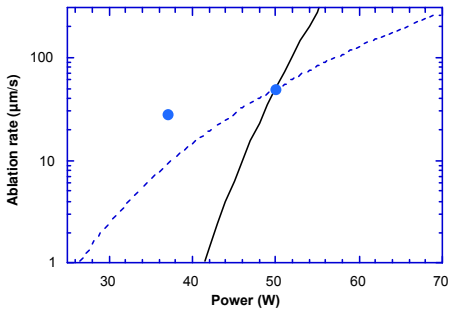

Fig.3: Ablation rate calculated with linear and nonlinear thermal is transport. Dots are experimental values. Solid line is calculated with linear thermal conduction, dotted line is calculated with thermal conductivity given by Eq.(5)

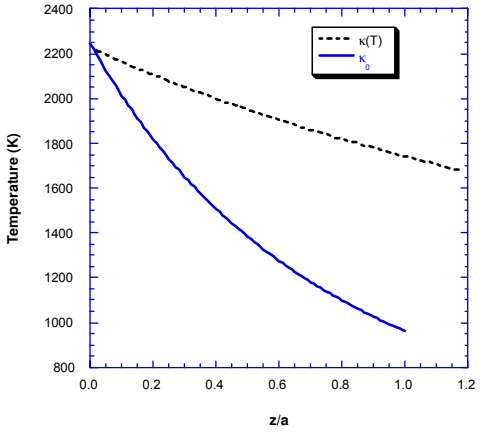

Fig.4: Temperature distribution vs. distance from the surface. Dashed line corresponds to temperature dependent thermal conductivity, solid line corresponds to constant thermal conductivity. Surface temperature of 2245 °K corresponds to the experimentally observed ablation rate of 50 µm/sec.

4. TEMPERATURE DISTRIBUTION

One must know the temperature distribution in the material to estimate the extent of the microcrack healing process. For the case of linear conduction and temporally flat top laser pulse, the temperature distribution is given by the expression

$$T(r,t)=\frac{Aa^2I}{D}\sqrt{\frac{\kappa}{\pi}}\int_0^t\frac{e^{\frac{-z^2}{4D t}}}{\sqrt{\tau}\left(a^2+4D\tau\right)}e^{-\frac{r^2}{a^2+4D\tau}}d\tau \tag{14}$$

At the center of the laser spot at r=0, the steady state temperature is given by the expression

$$T=\frac{AP}{(\pi)^{3/2}ak}\int_0^\infty\frac{e^{-\frac{z^2\varsigma^2}{a^2}}}{1+\varsigma^2}d\varsigma=\frac{AP}{2a\kappa_0\sqrt{\pi}}[1-erf[z/a]]e^{\frac{z^2}{a^2}} \tag{15}$$

When thermal conduction is nonlinear, however, according to the general result of the previous section we have

$$u(T)=\frac{AP}{2a\kappa_0\sqrt{\pi}}[1-erf[z/a]]e^{\frac{z^2}{a^2}} \tag{16}$$

for the quantity u defined in Eq.(11).

Temperature distributions for linear and nonlinear thermal conduction are shown in Fig.(4). One can see that the nonlinearity flattens the temperature distribution.

Typically, we are interested in cracks healing in a thin subsurface layer. For small z/a, by expanding Eq.(16) we obtain

$$T(z)=T_s-\frac{AP}{\pi a\kappa_0}(1+3\left(\frac{T_s}{T_0}\right)^3)^{-1}\frac{z}{a} \tag{17}$$

As already discussed, the steady state temperature onset takes a long time and in many situations the temperature evolution is nonstationary. In the linear regime the temperature evolution can be found from Eq.(14). To evaluate temperature in the nonlinear regime, we mention that we are mainly interested in rectification of a thin layer near the surface. On a short time scale, the temperature evolution can be treated by a 1D model and the expression Eq.(6) can be used for thermal conduction. The specific result for heat propagation in a medium with nonlinear heat conduction of form $\kappa=\beta T^n$ is the existence of a sharp temperature front with coordinate $z_f(t)$. Near the front the temperature variation behaves as

$$T=\left(\frac{nv}{\beta}\left|z-z_f\right|\right)^{1/n}$$

where v is the velocity of the thermal wave. The evolution of the temperature for the problem with fixed thermal flux q=AI on the boundary can be found from the following estimates[8].

For thermal conduction given by Eq.(6) the flux can be estimated as

$$q \sim \frac{\beta T^{n+1}}{z_f} = \frac{3\kappa_0 T_0}{z_f}\left(\frac{T}{T_0}\right)^4 \tag{18}$$

From the thermal conduction equation we have

$$T/t = q/z_f \tag{19}$$

From these relations we can find the temperature and thermal front coordinates

$$T = \frac{q^{\frac{1}{n+2}} t^{\frac{1}{n+2}}}{\beta^{\frac{1}{n+2}}} = q^{2/5} t^{1/5}\left(\frac{T_0^3}{3\kappa_0}\right)^{1/5}$$

$$z_f = \beta^{1/n+2} q^{\frac{n}{n+2}} t^{\frac{n+1}{n+2}} = \left(\frac{3\kappa_0}{T_0^3}\right)^{1/5} q^{3/5} t^{4/5}$$

Temperature increases relatively slowly. With propagation of the thermal front, the gradient drop and the temperature increase must satisfy conservation of the thermal flux.

5. MATERIAL REMOVAL

Heating of the surface induces material evaporation at a rate described by expression Eq.(4). The experimentally observed value is the crater depth

$$d = \int V dt \tag{20}$$

If the pulse duration is much longer than the thermal diffusion time, then the surface temperature is approximately equal to the steady state value T_s well before pulse termination and the crater depth is

$$d = V_0 e^{-\frac{U}{kT_s}} \tau$$

where τ is the pulse duration. For short pulses, when the temperature increases until the end of the pulse, the crater depth is determined mainly by the temperature at the end of the pulse $T(\tau)$. We can expand the temperature around $t=\tau$ to first order

$$T(t) = T(\tau) + T'(\tau)(t-\tau) \tag{21}$$

Calculating the integral in Eq.(20) we find

$$d = V_0 \frac{T(\tau)^2}{UT'(\tau)} e^{-\frac{U}{kT(\tau)}} \tag{22}$$

In both cases the depth is determined by the temperature at the end of the pulse and the dependence is exponential. A small change in temperature results in a large variation of depth. To increase the depth by a factor of e, one needs to vary the temperature by

$$\frac{\delta T}{T} = \frac{kT}{U} \approx 0.05$$

Thus, for linear thermal conduction, when temperature is proportional to laser power, a 5% variation of power will nearly triple the crater depth. For nonlinear thermal conduction, variations of power cause less extreme depth changes. For the thermal conductivity of Eq.(6), the variation of laser power must be four times larger to cause the same depth variation.

Since the evaporation rate is very temperature dependent, the steady state crater size can be estimated by expanding the surface temperature distribution of Eq.1) around r=0 and integrating over time. This yields a quadratic temperature distribution

$$T(r) = T_s (1 - r^2 / 2\, a^2)$$

Substituting this temperature distribution into the expression for the evaporation rate, Eq.(4), leads to an evaporation rate with Gaussian spatial shape. The 1/e radius of this evaporation rate is found to be

$$R = \sqrt{\frac{2kT_s}{U}}\, a$$

Thus, for the parameters given above, the crater radius is predicted to be 3 times smaller than the laser beam radius. This prediction is consistent with experimental observations.

In all our calculations, we disregarded cooling by evaporation. This is justified for the steady state regime[8]. For non-stationary processing, evaporative cooling can be important and would again make the processing less sensitive to power variations.

6. CRACK HEALING

The high-temperature induced by absorption of infrared radiation not only evaporates material, but also reduces the viscosity of fused silica so that surface tension is able to close cracks, thereby annealing the material and increasing its optical strength. As pointed out above, the increase of optical damage resistance after CO_2 laser processing has been known for several decades. What is new here is local application to heal specific defects.

The typical time τ for relaxation of a surface disturbance with scale l can be estimated from the hydrodynamics of an extremely viscous liquid[12] and is given by

$$\tau \sim \frac{\eta l}{\sigma} \qquad (23)$$

The surface tension σ for glass is about 300 dyne/cm[13] and not very sensitive to temperature. In the range of 1600-2000°C, the viscosity η is given by the expression[14]

$$\eta = 1.05 * 10^{-9} e^{\frac{E}{kT}} \quad poise \qquad (24)$$

where E is an activation energy, E~6.44 eV. For a deep crack, we must use the crack depth for *l*. If we know the crack depth and the acceptable annealing time, we can determine from Eqs.(23) and (24) the annealing temperature T.

We consider crack mitigation by local heating. The time for crack healing is given by Eq.(23). During this time d= Vτ of material will be ablated. The total amount of ablated material is given by the expression

$$d = \frac{\eta_0 l V_0}{\sigma} e^{\frac{E-U}{kT}} = 1.75 * 10^{-6} e^{\frac{32944}{T}}$$

Here d and *l* are in microns, T in degrees Kelvin. The numerical value is for a one-micron scale crack. The amount of material ablated during the crack healing process as a function of surface temperature is shown in Fig.(5). One can see that for the temperature 2245K used above, ablation of more than 4 μm guarantees that cracks in the subsurface layer will be annealed.

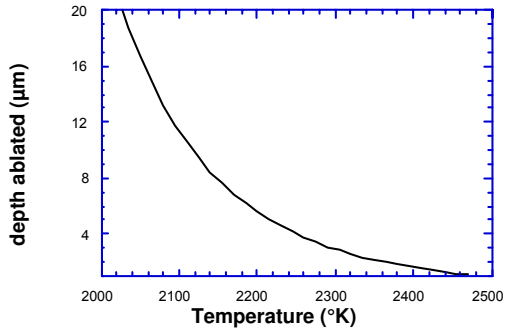

Fig.5: The amount of material ablated during the crack healing procedure.

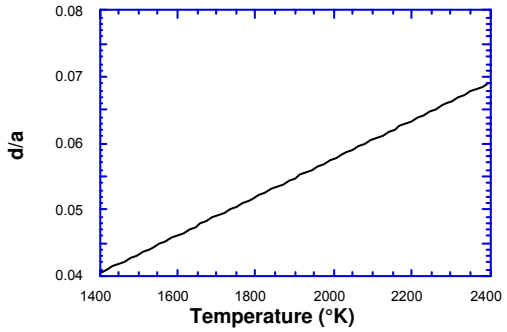

Fig.6: The thickness of the annealed layer as a function of the surface temperature.

Hence, in experiments[2] the laser-induced temperature must be high enough to heal the subsurface layer around the damage spot. Due to the nonlinearity of thermal conduction, the temperature distribution around the heated spot is reasonably flat and a wide zone of microcracks can be annealed.

We next estimate the extent of the annealed zone assuming the stationary temperature distribution. The temperature decrease inward into the heated material is given by Eq.(17), which can be rewritten as

$$T(z) = T_s - \delta T = T_s - \frac{2u'(T_s)}{u(T_s)\sqrt{\pi}} \frac{z}{a}$$

where u(T) is given by expression Eq.(11). The crack healing time is

$$\tau(z) = \tau(0) e^{\frac{E\delta T}{kT_s^2}} = \tau(0) e^{\frac{2EU(T_s)}{\sqrt{\pi} U'(T_s) kT_s^2} \frac{z}{a}}$$

and the thickness of the zone d in which cracks are healed is given by

$$d = \frac{\sqrt{\pi}\ kT_s^2 u'(T_s)}{2Eu(T_s)} a$$

The temperature dependence of d(T) is shown graphically in Fig.(6). For high temperatures

$$d \approx \frac{2\sqrt{\pi}\ kT_s}{E} a$$

For T_s =2245 K d~0.1a. One can see that the healing time is a strong function of the temperature while the thickness of the annealed layer is not very sensitive to surface temperature. If the crack is annealed near the surface, the thickness of the annealed layer will be thick enough to guarantee effective damage mitigation.

7. LASER INDUCED STRESSES

The laser-heated glass generates stress and strain due to thermal expansion. These strains can distort the initial flat glass surface, thus degrading the optical surface quality. Stresses can cause the glass to fail, producing cracks which act as centers for subsequent damage growth. The heated fused silica is soft and thermally-induced stresses are released by small material displacements. When the material cools, viscosity rapidly increases and material is then unable to move to further release stresses. The transition from "soft" to solid material is determined by many factors including the cooling rate. But due to the very strong viscosity temperature dependence, it is convenient to introduce the softening temperature T_{soft}. For temperatures below T_{soft} the stresses will be treated as imprinted into the material. For fused silica T_{soft} is 1585C.

One sees that if the heating of the glass is stationary, i.e. v<D/a where v is the scan velocity and D the thermal diffusivity, the time for buildup of stresses is τ_σ~a/s (s is the sound speed). This time is much smaller than the time to scan over the spot a/v~a^2/D. In this regime, stresses and strains can be treated as stationary.

To make an estimate, consider a model spherically symmetrical temperature distribution T(r). At large r, for steady state temperature distribution, the heat equation gives T ~T_0a/r. The temperature gradually drops from T~T_0 at the spot center with spatial scale ~a. The material displacement u in this case has only a radial component $u_r(r)$ =u(r) given by

$$u = \alpha \frac{1+\nu}{(1-\nu)} \frac{1}{r^2} \int_0^r T(r) r^2 dr$$

Here α=7*10^{-7} °K^{-1} is the linear thermal expansion coefficient; υ=0.17 is the Poisson ratio. The maximum displacement occurs at r~a where u~αTa. That is, the displacement is proportional to the spot size. For T~2000 °K and a=1mm, this displacement is about 1 μm. The residual deformation remaining after the glass freezes can be expected to be of the same order because of the high viscosity. It is clear that deformations of this scale can seriously affect the part's optical quality. The danger to surface quality for large-area scanning is apparent.

The resulting strains and stresses can be calculated from the above displacement u
Strains:

$$u_{\theta\theta} = u_{\varphi\varphi} = \frac{u}{r}$$
$$u_{rr} = \frac{\partial u}{\partial r} = -2\frac{u}{r} + \frac{\alpha(1+\nu)}{(1-\nu)} T(r) \qquad (25)$$

Stresses

$$\sigma_{ik} = \frac{E}{1+\nu}\left(u_{ik} + \frac{\nu}{1-2\nu}u_{ll}\delta_{ik}\right)$$

Here E is Young's modulus, E=74 GPa for fused silica
Hoop tensile stresses are the most dangerous:

$$\sigma_{\theta\theta} = \frac{\alpha E}{(1-\nu)(1-2\nu)}\left((1-2\nu)\tilde{T}(r) + \nu T(r)\right) \qquad (26)$$

$$where \quad \tilde{T} = \frac{\int_0^r T(r) r^2 dr}{r^3}$$

Maximal hoop stress occurs at r~a and is given by

$$\sigma \sim \alpha E T \qquad (27)$$

Hoop stress is independent of beam size and for T~2000 °C, σ~0.1GPa which is comparable with the silica tensile strength~0.05 GPa. Of course, we cannot conclude that the silica will inevitably crack as a result of processing. These estimates are uncertain by a factor of a few. Also, the maximum stress occurs where the glass is hot and ductile, cracking takes place during the cooling stage when thermal gradients are somewhat smoothed so stresses at that point will be smaller. But the above estimate does point out the possibility of cracking during the mitigation process.

To open a crack of length l, one must apply the stress $\sigma=K/\sqrt{l}$, where K is the toughness of the material. K=0.75 MPa $m^{1/2}$ for fused silica. The stress amplitude is determined by the maximum temperature only, but the extent of the zone of the maximal stress is about equal to the spot size. Hence, mitigation with a bigger spot size and the same peak temperature is more dangerous in terms of cracking.

The previous discussion deals with the steady state temperature distribution. As discussed above, the stresses are relaxed in hot material, and imprinted only when the temperature drops to $T=T_{soft}$. At this moment, the temperature distribution extends a large distance and the initial temperature distribution can be treated as a point source

$$T=B\delta(r) \qquad (28)$$

The constant A can be found from the energy balance

$$\rho c \int T(r) dV = AP\tau; \qquad B = 2\frac{AP\tau}{\rho c}$$

The initial distribution in Eq.(28) evolves in time as

$$T(r,t) = \frac{B}{8(\pi D t)^{3/2}} e^{-\frac{r^2}{4Dt}}$$

When the temperature in the center is equal to T_{soft} the typical size of the distribution is

$$(4Dt)^{1/2} = \left(\frac{B}{T_{soft}}\right)^{1/3} = \left(\frac{AP\tau}{\rho c T_{soft}}\right)^{1/3} \quad (29)$$

For stress calculations, one can use Eqs.(25)-(28). The value of the imprinted hoop stress is

$$\sigma \sim \alpha E T_{soft}$$

and the size of the stressed zone is given by Eq.(29)

8. SUMMARY

We have presented above an analysis of thermal processes associated with laser mitigation of damaged spots. The results are a semi-quantitative description of the mitigation process, including some possible pitfalls.

•We obtained scalings which can, in principle, relate experiments with operational parameters. The main conclusions of the analysis are in good correlation with recent experiments[15].
•The observed pit depth is predicted to be very sensitive to process parameters due to the strong dependence of evaporation rate on temperature.
•Best results were predicted for processing with short pulses. Surface temperature will be higher for short pulse mitigation, and this also aids crack healing.

There are some effects left out of our description. We disregarded the melt motion under the effect of reciprocal momentum produced by evaporation. Also we didn't take into account the cooling due to evaporation. For typical mitigation parameters, these effects are not expected to be important[8], but may play a role for short, intense pulses when the surface temperature is high.

Finally, we note that the experiments[6,15] reveals noticeable debris deposition around the processed spot. The nature and the effect of this debris on damage need additional study.

ACKNOWLEDGEMENTS

This work was performed under the auspices of the U.S. Department of Energy by University of California, Lawrence Livermore National Laboratory under Contract W7405-Eng.48.

9. REFERENCES

1. M.A. Norton, L.W. Hrubesh, Z. Wu, E.E. Donohue, M.D. Feit, M.R. Kozlowski, D. Milam, K.P. Neeb, W.A. Molander, A.M. Rubenchik, W.D.. Sell and P. Wegner, "Growth of laser initiated damage in fused silica at 351 nm", *Laser-Induced Damage in Optical Materials: 2000* , Proc. SPIE **4347,**. 468-468 (2001).

2. L.W.Hrubesh, M.A.Norton, W.A.Molander, E.E.Donohue, S.M.Maricle, B.M.Penetrante, R.M.Brusasco, W.Grundler, J.A.Butler, J.W.Carr, R.M.Hill, L.J.Summers, M.D.Feit, A.Rubenchik, M.H.Key, P.J.Wegner, A.K.Burnham, L.A. Hackel and M.R.Kozlowski, "Methods for mitigating surface damage growth on NIF final optics", *Laser-Induced Damage in Optical Materials: 2001*, Proc. SPIE **4679**, (2002).

3. P. A. Temple, D. Milam and W. H. Lowdermilk, “CO2 laser polishing of fused silica surfaces for increased laser damage resistance at 1.06 μm”,Nat. Bur. Stand. (U.S.) *Spec. Publ*. **568,** 229-36 (1979).
4 . P. A. Temple and M. J. Soileau,” 1.06 nm laser-induced breakdown of CO2-laser-polished fused SiO2”, Nat. Bur. Stand. (U.S.) *Spec. Publ*. **620**, 180-89 (1981).
5. P.A. Temple, W.H. Lowdermilk, D. Milam, “Carbon dioxide laser polishing of fused silica surfaces for increased laser-damage resistance at 1064 nm”, *Appl. Opt*. **21**, 3249-55 (1982).
6. P. A. Temple, S. C. Seitel, and D. L. Gate,” CO2 Laser Polishing of Fused Silica: Recent Progress”, Nat. Bur. Stand. (U.S.) *Spec. Publ*. **669**, 130-37 (1984).
7. T. Raj, D. E. McCready and C. K. Carniglia ,”Substrate Cleaning in Vacuum by Laser Irradiation, ”NIST (U.S.) *Spec. Publ*. **775,** 152-64 (1989).
8. M.D. Feit and A.M. Rubenchik, "Glass polishing by CO2 laser", LLNL memo NIF-0059084 (December 13, 2000).
9. M.Bass, “Laser-materials interactions”, in *Encyclopedia of Lasers and Optical Technology*, R.Meyers, ed., *Academic Press*, (San Diego,1991).
10. S.I. Anisimov, V.A.Khokhlov, "Instabilities in Laser-matter interaction", *CRC Press* (1999).
11. H.Schoize, *Glass*, Springer-Verlag (1991).
12. H.Lamb," Hydrodynamics", *Dover Publications*, (New York 1945), pp. 624-626.
13. "The Handbook of Glass Manufacture", 3rd ed.v.2, p.930 *Ashlee Publishing Co*. (N.Y. 1984).
14. D.Hewak, Ed., "Properties, processing and applications of glass and rare earth-doped glasses for optical fibres", *INSPEC* (London, 1998).
15. W.Molander, “Laser parameter optimization and process design for CO_2 laser mitigation of fused-silica optics”, LLNL memo NIF-0075949 (January 16,2002).